

# Vortices and Dissipation in a Bilayer Thin Film Superconductor

Wei Zhang and H. A. Fertig

*Department of Physics, Indiana University, Bloomington, IN 47405*

(Dated: September 29, 2018)

## Abstract

Vortex dynamics in a bilayer thin film superconductor are studied through a Josephson-coupled double layer XY model. A renormalization group analysis shows that there are three possible states associated with the *relative* phase of the layers: a free vortex phase, a logarithmically confined vortex-antivortex pair phase, and a linearly confined phase. The phases may be distinguished by measuring the resistance to counterflow current. For a geometry in which current is injected and removed from the two layers at the same edge by an ideal (dissipationless) lead, we argue that the three phases yield distinct behaviors: metallic conductivity in the free vortex phase, a power law I-V in the logarithmically confined phase, and true dissipationless superconductivity in the linearly confined phase. Numerical simulations of a resistively shunted Josephson junction model reveal size dependences for the resistance of this system that support these expectations.

PACS numbers: 74.78.-w, 64.60.-i, 75.10.Hk

Keywords: KT transition, vortices deconfinement

## I. INTRODUCTION

Topological defects play an important role in many condensed matter systems. A paradigm of this are vortices in systems whose energetics may be described by a single angular variable  $\theta(\mathbf{r})$  that is a function of position  $\mathbf{r}$ , the simplest example being an  $XY$  magnet (also known as the planar rotor model [1].) The state of the vortices in two-dimensional systems determines important physical properties. For example, at high temperatures free vortices in superfluid films and thin film superconductors lead to dissipation. At low temperatures, the defects are bound into vortex-antivortex (VAV) pairs, yielding a state with power-law (quasi-critical) behavior in the correlation function  $\langle e^{i\theta(\mathbf{r})} e^{-i\theta(0)} \rangle$ . While neither the bound nor the unbound vortex phase supports long-range order [2], there is a well-known thermodynamic phase transition – the Kosterlitz-Thouless transition [3] – in which the vortices unbind at a critical temperature  $T_{KT}$ .

The situation is dramatically changed when one introduces an explicit symmetry-breaking field that aligns the angles (such as a magnetic field in the  $XY$  model). One of us [4, 5, 6] investigated this situation recently and found that the vortices have *three* possible phases: a free vortex phase, a logarithmically bound VAV pair phase, and a linearly confined phase. Can these phases be distinguished in an experimental system described by this model? This is the issue we address in this paper.

The problem of the resistive transition in a single layer superconductor was studied in Ref. 7. It was found that for  $T > T_{KT}$ , a current produces a force on a free vortex, whose subsequent motion then induces a voltage along the direction of current. This produces a linear  $I - V$  curve. For  $T < T_{KT}$ , bound VAV pairs have no *net* force on them due to a current and so create no net voltage drop. A voltage is induced by unbound vortices, but these are only induced by the current, leading to a non-linear (power law)  $I - V$  curve at low currents. In this work, we study the analog of this for a system with explicit symmetry-breaking: the voltage response of a Josephson-coupled bilayer thin film superconductor with respect to an injected counterflow current. As discussed below, the Josephson coupling acts as an explicit symmetry-breaking for the *relative* phase of the order parameters for the two layers,  $\theta_1(\mathbf{r}) - \theta_2(\mathbf{r})$ . Isolated vortices in the relative phase respond to currents in *opposite* directions in the two layers, and their motion induces an interlayer voltage. Thus, to probe vortices in the relative phase, current must run in opposite directions in the two layers; i.e., we must have a counterflow current. A geometry in which this is induced results when current is injected in one layer and removed from the other at the *same* edge of the sample, which to our knowledge was first studied by Ferrell and Prange [8], in the absence of vortex excitations. In this situation, the current penetrates the system up to a characteristic length scale – the Josephson length – set by the tunneling matrix element and the superfluid stiffness

of the layers. Unlike the case for current in an individual layer, the counterflow current can decay because an injected charge carrier in the top layer can tunnel to the bottom layer, and exit the system on the same edge of the bilayer from which it entered.

As we show below, when vortices are introduced, their dynamics generates different behavior for the three phases: metallic conductivity in the free vortex phase, a power law  $I - V$  in the logarithmically confined phase, and true dissipationless superconductivity (zero resistance at finite current) in the linearly confined phase. This last phase is qualitatively different from anything that occurs for the voltage response of a single superconducting layer. As we demonstrate via simulation below, by measuring the voltage difference between the two layers at a single edge, we may distinguish the three phases.

The organization of this paper is as follows. In Section 2, we introduce our model and map it to a Josephson coupled bilayer XY model. In Section 3, the phase diagram is studied by duality transformation and a renormalization group (RG) analysis. Section 4 discusses the  $I - V$  curves and finite system effects. The numerical simulations are presented in Section 5, and we conclude with a summary.

## II. THEORETICAL MODEL

We consider a bilayer thin film superconductor, which can be described by a form of the Lawrence-Doniach (LD) model [9]. The LD free energy may be written as

$$\mathcal{F} = \int d^2r \sum_{n=1,2} \left\{ A|\psi_n|^2 + \frac{B}{2}|\psi_n|^4 + 2\alpha|\nabla\psi_n|^2 + h \cos(\theta_1 - \theta_2) \right\}, \quad (1)$$

where  $\psi_1 = |\psi_1|e^{i\theta_1}$ ,  $\psi_2 = |\psi_2|e^{i\theta_2}$  are the order parameters for the two layers with coordinates  $\mathbf{r} = (x, y)$ , and the last term is the Josephson coupling between the two layers. Neglecting fluctuations of  $|\psi_n|$ , we obtain a free-energy functional with only the phases involved,

$$\begin{aligned} \mathcal{F} &= \int d^2r \left\{ 2\alpha(\nabla\theta_1)^2 + 2\alpha(\nabla\theta_2)^2 + h \cos(\theta_1 - \theta_2) \right\} \\ &= \int d^2r \left\{ \alpha[\nabla(\theta_1 + \theta_2)]^2 + \alpha[\nabla(\theta_1 - \theta_2)]^2 + h \cos(\theta_1 - \theta_2) \right\}. \end{aligned} \quad (2)$$

The free-energy  $\mathcal{F}$  does not support vortex excitations, because in neglecting variations in the amplitudes of  $|\psi_i|$  we did not allow for the zeros that are necessarily contained in their cores. To reintroduce these, we replace  $\mathcal{F}$  with a free energy functional  $F$  whose degrees of freedom are defined on a (square) lattice. By making the replacement  $1 - \frac{1}{2}\theta^2 \rightarrow \cos(\theta)$ , we allow for configurations in which plaquettes of the square lattice may contain a non-vanishing vorticity. The resulting free-energy, which has a form similar to what expects for

a bilayer Josephson junction array, is

$$F = \alpha \sum_{\langle r, r' \rangle} \cos[\theta_1(r) - \theta_1(r')] + \alpha \sum_{\langle r, r' \rangle} \cos[\theta_2(r) - \theta_2(r')] - h \sum_r \cos[\theta_1(r) - \theta_2(r)], \quad (3)$$

where  $\langle r, r' \rangle$  refers to nearest neighbor sites. Models of this form have been studied previously in [10].

The analysis of  $F$  is complicated by the fact that, in computing the partition function  $Z = \int \mathcal{D}\theta e^{-F}$ , there are cosines appearing in the exponential. As is well-known [1, 11], considerable progress can be made if we replace the Josephson coupling form of the partition function with a Villain model [12]. This essentially involves replacing  $e^{J \cos \theta}$  with  $\sum_{m=-\infty}^{\infty} e^{-J(\theta - 2\pi m)^2/2}$  wherever it appears in the partition function. The replacement works because the effective weighting has the same periodicity as the original Josephson coupling form, so that we should retain the same possible phases for the system [1]. We obtain an important simplification by replacing a cosine form with a Gaussian weighting because it ultimately allows one to integrate out the angular degrees of freedom [11]. The cost, however, is the introduction of effective integer degrees of freedom, which with some work can be understood in terms of the vortex excitations of the system [4, 11]. Following a standard trick for rewriting the partition function as a sum over dual degrees of freedom [4, 11], we find the partition function for the Villain form of the free energy may be written as  $Z = \sum_{\mathbf{S}, T} e^{-F_{VM}[\mathbf{S}, T]} \prod_r \delta(\nabla \cdot \mathbf{S}_1(r) - T(r)) \delta(\nabla \cdot \mathbf{S}_2(r) + T(r))$ , with

$$F_{VM}[\mathbf{S}] = \frac{1}{2\alpha} \sum_r [\mathbf{S}_1^2(r) + \mathbf{S}_2^2(r)] + \frac{1}{2h} \sum_r T^2(r), \quad (4)$$

where  $\mathbf{S}_{1,2}$  are integer fields lying on the bonds of the lattice in each layer, and  $T$  is an integer field defined on the lattice sites.

### III. VORTEX PHASE DIAGRAM

A useful representation [4, 5] of the bond degrees of freedom may be written as  $S_{1x} = \partial_y m$ ,  $S_{1y} = -\partial_x m - A$ ,  $S_{2x} = \partial_y n$ ,  $S_{2y} = -\partial_x n + A$ , where  $n$ ,  $m$ , and  $A$  are all integer fields. In terms of these the effective free energy  $F_D$  for the partition function  $Z = \sum_{m, n, A} e^{-F_D}$  is

$$F_D = \frac{1}{2\alpha} \sum_r |\nabla m(r) + A(r)\hat{x}|^2 + \frac{1}{2\alpha} \sum_r |\nabla n(r) - A(r)\hat{x}|^2 + \frac{1}{2h} \sum_r \left(\frac{\partial A}{\partial y}\right)^2. \quad (5)$$

As has been discussed elsewhere, the single layer version of this – in which the middle term of 5 is essentially absent – may be understood as a model of an interface, with domain walls and screw dislocations [4]. In that situation the  $m$  field allow us to represent configurations with closed domain walls, and the  $A$  field introduces open domain wall configurations. For  $F_D$ , we have closed domain wall configurations separately introduced in each layer by the  $m$ ,  $n$

fields, and the  $A$  field, rather than completely eliminating sections of closed domain walls as in the single layer case, here allows it to shift between the two layers. Because of their close analogy, we will call these “kinks” in the domain walls dislocations in the remainder of this paper. Physically, the domain walls may be interpreted as worldline trajectories for Cooper pairs, and the dislocations represent interlayer tunneling events.

One advantage of this representation is that the coupling constants are the inverse of those in the original functional. This strong-weak duality makes it convenient to study the physics with strong inter-layer coupling. We can obtain further insight by looking at the problem in the vortex representation. To do this, we apply the Poisson resummation rule [11] on the integer fields  $m$ ,  $n$ , and arrive another representation of the partition function in terms of integer fields  $M$ ,  $N$  and  $A$ . The energy functional associated with these degrees of freedom is

$$F_V = - \sum_q \frac{2\pi^2 K}{S} \frac{|M + N|^2}{|\mathbf{Q}|^2} - \sum_q \frac{2\pi^2 K}{S} \frac{|H|^2}{|\mathbf{Q}|^2} - \sum_q \left( \frac{1}{2KS|\mathbf{Q}|^2} + \frac{1}{2h} \right) |Q_y|^2 |A(\mathbf{q})|^2 - \frac{2\pi i}{S} \sum_q \frac{(Q_x)}{|\mathbf{Q}|^2} A(\mathbf{q}) H^*(\mathbf{q}), \quad (6)$$

where  $S$  is the number of lattice sites,  $M$  and  $N$  are the vortex numbers for the two layers,  $H = M - N$ ,  $K = \alpha/2$ ,  $\mathbf{Q} = (Q_x, Q_y)$ , and  $Q_x = 1 - e^{-iq_x a}$ ,  $Q_y = 1 - e^{-iq_y a}$ , with  $a$  the lattice constant. Physically, we understand the  $M + N$  integer field as the vortices of the symmetric combination of the original layer phases, whereas  $H$  represents vortices for the antisymmetric combination. Comparing the terms involving  $H$  with Eq. 12 in Ref. 5, we see that the energetics of anti-symmetric vortices are identical to those of the single layer  $XY$  model with external magnetic field. It is thus not surprising that the phases of this system are analogous to those found in the latter problem.

It is useful to note that in the representation of Eq. 6, the partition function shows a near duality. This can be seen more clearly if one defines  $J(\mathbf{q}) = Q_y A(\mathbf{q})$ . In real space  $J$  is also an integer field, and if one eliminates  $A$  in favor of  $J$  in Eq. 6, then a near symmetry is apparent under interchange of  $J$  and  $H$  and  $K \rightarrow 1/4\pi K$  in  $F_V$ . To fully exploit this symmetry, we add a term of the form  $E_c \sum_q |H(\mathbf{q})|^2$ , after which the duality ( $K \rightarrow 1/4\pi K$ ,  $E_c \leftrightarrow 1/h$ ) becomes exact [11]. The integer fields  $H$  and  $J$  may be respectively interpreted as the vortex field and a dislocation field, with the added  $E_c$  term representing a core energy for vortices. The duality in this representation shows that if we can determine what happens to the dislocations in one part of the phase diagram, we will know what happens to the vortices in another.

To proceed with finding the phases of this system, we need to perform an RG analysis. To do this, we wish to work with continuous rather than integer degrees of freedom. Following the standard reasoning that the phases depend on the symmetries of the Hamiltonian and

not the precise form of the degrees of freedom [13], we replace the partition function with one of the form  $Z_{eff} = \int \mathcal{D}\theta \int \mathcal{D}\phi \int \mathcal{D}a e^{-H_{eff}}$ , with

$$H_{eff} = \int d^2r \frac{1}{2\alpha} |\nabla\phi_1 + a\hat{x}|^2 + \frac{1}{2\alpha} |\nabla\phi_2 - a\hat{x}|^2 + \frac{1}{2h} \left(\frac{\partial a}{\partial y}\right)^2 \quad (7)$$

$$(-y_{\phi_1} \cos 2\pi\phi_1 + y_{\phi_1}) + (-y_{\phi_2} \cos 2\pi\phi_2 + y_{\phi_2}) + (-y_a \cos 2\pi a + y_a).$$

Here the last three terms are added to favor configurations in which  $\phi_{1,2}$  and  $a$  are integers. The parameters  $y_{\phi_{1,2}}$  have the physical interpretation of fugacities for vortices in the individual layers, and for small values they favor configurations with vorticity  $(0, \pm 1)$  in each plaquette. The parameter  $y_a$  can be understood as a core energy for a kink of a domain wall into one layer from the other, and as has been discussed elsewhere [5] should be taken proportional to  $1/h$  to match the energetics of such kinks in the domain wall model  $F_D$ .

To identify the phases of the vortex system, we wish to find the fixed points to which  $H_{eff}$  flows under the RG. We write the effective Hamiltonian as  $H_{eff} = H_0 + H_1$ , with the unperturbed Hamiltonian

$$H_0 = \int d^2r \frac{1}{2\alpha} |\nabla\phi_1 + a\hat{x}|^2 + \frac{1}{2\alpha} |\nabla\phi_2 - a\hat{x}|^2 + \frac{1}{2h} \left(\frac{\partial a}{\partial y}\right)^2 + \frac{1}{2}\rho a^2 \quad (8)$$

with initial value  $\rho(\ell = 0) = 2\pi y_2(\ell)$ , and

$$H_1 = (-y_{\phi_1} \cos 2\pi\phi_1 + y_{\phi_1}) + (-y_{\phi_2} \cos 2\pi\phi_2 + y_{\phi_2}) + \sum_{n=2}^{n=\infty} \frac{y_{2n}}{2^n n!} (-1)^n (2\pi a)^{2n} \quad (9)$$

with the initial values  $y_{2n}(\ell = 0) = y_a$ . (Here  $e^\ell$  represents the length scale to which the degrees of freedom have been integrated out in the RG.) We perform the RG perturbatively in  $H_1$ ; since  $y_a \sim 1/h$ , this amounts to looking at the RG flows in the region of a strong coupling fixed point.

To lowest order in  $y_{\phi_1}$ ,  $y_{\phi_2}$ , and  $y_a$ , the RG flow equations can be shown to take the form [5]

$$\begin{aligned} \frac{dy_{\phi_1}}{dt} &= (2 - \pi K \sqrt{\frac{1 + K\rho}{K\rho}}) y_{\phi_1} \\ \frac{dy_{\phi_2}}{dt} &= (2 - \pi K \sqrt{\frac{1 + K\rho}{K\rho}}) y_{\phi_2} \\ \frac{dy_{2n}}{dt} &= -(2n - 2) y_{2n} - 2\pi^2 L(\rho, \xi) y_{2n+2} \\ \frac{d\rho}{dt} &= -8\pi^4 L(\rho, \xi) y_4, \end{aligned} \quad (10)$$

where (for  $\rho \ll 1$ )

$$L = \frac{K\xi}{\pi \sqrt{K\rho(1 + \xi\Lambda)}} \quad (11)$$

with  $\Lambda = \pi/a$  and  $\xi = \sqrt{K/h}$ . We note that since  $\rho$  is small throughout the flow range, the vortex fugacities  $y_\phi$  and  $y_\theta$  are strongly irrelevant, indicating that vortices are always

bound in both layers for the parameter regime where our calculations apply, large vortex core energies and small  $1/h$  (i.e., *large* symmetry-breaking field.) This may seem at first surprising, since we expect that “symmetric” vortices (i.e., the combination  $M+N$  in vortex free energy, Eq. 6) should undergo a Kosterlitz-Thouless transition. This is true, but in our formulation it can be found only at order  $y_{\phi_1}y_{\phi_2}$  because this involves creating vortices in *both* layers at a given position. In the domain wall representation, this corresponds to an operator of the form  $y_{\phi_1+\phi_2} \int d^2r \cos[\phi_1(\mathbf{r}) + \phi_2(\mathbf{r})]$  becoming relevant, so that closed “double” domain walls – closed domain walls lying in both layers at the same time – cannot proliferate for the parameters corresponding to the unbound symmetric vortex state. At our order in perturbation theory this has no effect, nor do we expect it to qualitatively: since “single” domain walls (i.e., closed domain walls in a single layer, generated by either  $\phi_1$  or  $\phi_2$ ) are proliferated, the presence or absence of these higher order domain walls should not affect the qualitative physics of single vortex unbinding.

The “mass” parameter  $\rho$  plays a crucial role in determining the meaning of the fixed point Hamiltonian. If  $\rho \rightarrow 0$  then the field  $a$  may effectively remove arbitrarily large sections of the closed domain wall sections generated by fluctuations in the fields  $\phi_1$  and  $\phi_2$ . This corresponds to an unbound phase of dislocations. When  $\rho > 0$ , it becomes prohibitively expensive energetically to remove large domain wall segments, and the dislocations remain bound. Thus, the initial parameters that divide trajectories for which  $\rho(\ell \rightarrow \infty) > 0$  from those in which  $\rho(\ell \rightarrow \infty) = 0$  represent a boundary separating states in which dislocations are paired or deconfined [4, 5]. The flow equations 10 have been studied in detail in Refs. 4 and 5, and they demonstrate that a transition from  $\rho = 0$  to  $\rho > 0$  at the fixed point indeed occurs for a critical value of  $y_a$ ; i.e., a critical value of  $h$ . Thus, for arbitrarily small vortex fugacity, there is a dislocation unbinding transition at a critical value of the symmetry-breaking field,  $h_c$ , with the unbound state on the small  $h$  side of this, and the bound state on the large  $h$  side.

Because of the duality between vortices and dislocations, *this implies there must also be a vortex unbinding transition.* The duality suggests that the unbound vortex phase should occur for small  $h$  and small  $E_c$ , as one might intuitively expect. There are then three possible phases for the system, an unbound vortex phase and two bound phases, the latter being distinguished by whether dislocations are in a bound or unbound state. As has been discussed in Ref. 5, these two phases may be described in terms of the vortex degrees of freedom by whether the VAV pairs are linearly confined, or logarithmically bound. The linearly confined phase may be understood as the natural situation for very dilute vortices. Returning to the original XY model with a symmetry-breaking field, a state with a single high separated VAV pair has its energy minimized by creating a string of overturned angle with finite width of order  $\xi$  connecting the two topological defects [14]. (For separations

smaller than this, the interaction energy is approximately logarithmic, as in the absence of the symmetry-breaking field.) This string arises because the symmetry-breaking field introduces a large energy cost for states in which the phase deviates from  $\theta = 0$  over a large area. Since a vortex requires a  $2\pi$  angular rotation for any path surrounding its core, one minimizes the loss in interaction energy with the field by confining the rotation to a narrow region. These strings may be understood as a degree of freedom dual to the domain walls that arose in the dislocation representation.

The interpretation of the  $\rho > 0$  phase comes in part from noticing that  $y_\phi$  is irrelevant, so that domain walls are proliferated by thermal fluctuations. Because of the duality, we expect the same to be true for the strings in the vortex representation of this state. Physically, this means the entropy of the strings overwhelms their energy, so that strings of arbitrarily large size may be found in a typical configuration. However, the *logarithmic* attraction between VAV pairs is not screened by the proliferating strings, so they remain bound within the intermediate phase. Vortex unbinding only occurs at higher temperatures and/or lower  $E_c$  and/or lower  $h$  when the entropy overcomes the logarithmic interaction. A detailed discussion of how the RG analysis leads to this picture in the single layer case may be found in Ref. 5.

Finally, we note that the existence of all three phases has been demonstrated in the  $XY$  model with a magnetic field using a simulation method that directly probes the fluctuations of the vortices.

#### IV. VORTEX EFFECTS IN COUNTERFLOW RESISTANCE

In this section, we discuss how the different vortex phases could be distinguished in a transport experiment. Because the system will contain “double” vortices (pairs of vortices stacked across the layers) which behave in a fashion similar to vortices in a single layer system, deconfinement of single vortices would be difficult to see in a measurement the  $I - V$  curve of the bilayer film as a whole. The problem of competing effects due to double vortices can be overcome if we consider a *counterflow* current, which creates forces on a single vortex but not on a double vortex. We thus consider a geometry in which the current  $J$  is injected and removed in the  $\hat{x}$ -direction from the two layers at the same edge (see Fig. 1). The current distribution in such an experiment has been analyzed in the absence of vortices and other fluctuations [8], where it was found that the current within each layer  $j_x$  and the interlayer (tunneling) current  $j_z$  behave as  $j_x \sim \text{sech}(x/\lambda_J)$  and  $j_z \sim \text{sech}(x/\lambda_J)\tanh(x/\lambda_J)$  with  $\lambda_J = \sqrt{K/\hbar}$  the Josephson length. These currents are non-vanishing within a strip of width  $\sim \lambda_J$ , so that vortices entering this region will be subject to forces due to the current.



To simplify the analysis below, we will model this by a uniform tunneling current within  $\lambda_J$  of the edge, and take the currents to be zero deeper inside the sample.

To understand qualitatively the impact of the vortices, consider one vortex in the relative phase field  $\Phi = \theta_1 - \theta_2$ . This configuration can be realized as  $(M, N) = (1, 0)$  or  $(0, -1)$ , where  $(M, N)$  is the vortex number in each layer (see Eq. 6). For  $(M, N) = (1, 0)$ , there is one vortex in the upper layer, and none in the lower layer. Suppose the current is directed in the lower layer so that the resulting motion of the vortex generates a voltage  $+V$  relative to that in the middle of the system, where we choose the electric potential to be zero. For a single vortex of the form  $(M, N) = (0, -1)$ , the vortex will move in the same direction as in the previous case because both the direction of current in the relevant layer and the vorticity have changed sign. Since this creates a vortex current of the *opposite* sign of that found in the upper layer, the voltage generated in that layer will have the same magnitude on average but opposite sign,  $-V$ . Thus, any vortex current induced by the counterflow current produces an interlayer voltage at the edge.

To analyze this in detail, we adopt the approach of Ambegaokar et al. described in Ref. 15, which we hereafter refer to as AHNS. AHNS demonstrated that the dynamics of vortices in response to a driving current, and the voltage they induce, may be described using a Fokker-Planck equation. In this approach, the separation  $r$  of a VAV pair is described by the stochastic differential equation

$$\frac{dr}{dt} = -\frac{2D}{k_B T} \frac{\partial U}{\partial r} + \eta(t), \quad (12)$$

where  $U$  is the effective potential for a VAV pair,  $D$  is the diffusion constant, and  $\eta(t)$  represents the thermal noise, with the correlation function  $\langle \eta(t)\eta(t') \rangle = 4D\delta(t-t')$ . Since the vortices of interest are located in a strip of width  $\lambda_J$  near the system edge, we will in fact solve a one dimensional problem. From the above stochastic differential equation, one obtains a Fokker-Planck equation, describing the relation between  $\Gamma(y)$ , the number density of VAV pairs near the edge with vertical separation  $y$ , and the vortex current density  $I$ . One may start from

$$\Gamma(y, t + \Delta t) = \int dy' P(y, t + \Delta t | y', t) \Gamma(y', t), \quad (13)$$

where  $P(y, t + \Delta t | y', t) = \langle \delta(y - y(t + \Delta t)) \rangle_{y't}$  is the probability for a VAV pair having separation  $y$  at time  $t + \Delta t$ , given that it had separation  $y'$  at time  $t$ . From Eq. (12) one has

$$y(t + \Delta t) = y' - \frac{2D}{k_B T} \frac{\partial U}{\partial y} \Delta t + \int_t^{t+\Delta t} \eta(t_1) dt_1 \quad (14)$$

Expanding  $P(y, t + \Delta t | y', t)$  to first order in  $\Delta t$ , we obtain

$$P(y, t + \Delta t | y', t) = \left[ 1 - \frac{2D}{k_B T} \frac{\partial U}{\partial y} \Delta t \frac{\partial}{\partial y'} + \frac{1}{2} \int_t^{t+\Delta t} dt_1 \int_t^{t+\Delta t} dt_2 \langle \eta(t_1)\eta(t_2) \rangle \frac{\partial^2}{\partial y'^2} \right] \delta(y - y') \quad (15)$$

Making use of the fact that  $\int_t^{t+\Delta t} dt_1 \int_t^{t+\Delta t} dt_2 \langle \eta(t_1)\eta(t_2) \rangle = 4D\Delta t$  and integrating by parts in Eq. 13, one can obtain

$$\frac{\partial \Gamma}{\partial t} = \frac{\partial}{\partial y} \left( \frac{2D}{k_B T} \Gamma \frac{\partial U}{\partial y} + 2D \frac{\partial \Gamma}{\partial y} \right), \quad (16)$$

which may be rewritten as

$$\frac{\partial \Gamma(y)}{\partial t} = -\frac{\partial}{\partial y} I. \quad (17)$$

with

$$I = -2D \exp\left(\frac{-U}{k_B T}\right) \frac{\partial}{\partial y} \left[ \Gamma(y) \exp\left(\frac{U}{k_B T}\right) \right]. \quad (18)$$

For a steady-state solution,  $I$  is a constant and has the interpretation of the number of separating pairs per unit time; i.e. the generation rate for free vortices. The concentration of unbound vortices  $n_f$  is determined by the balance equation

$$\frac{dn_f}{dt} = I - \beta n_f^2. \quad (19)$$

In this equation, the first term represents a generation rate for unbound VAV pairs, while the second term is due to vortex recombination. In steady state ( $\frac{dn_f}{dt} = 0$ ),  $n_f \sim \sqrt{I}$ . Finally, we note that the interlayer voltage is generated by a net vortex current, and so is proportional to the density of free vortices. Thus we have  $\rho \sim n_f \sim \sqrt{I}$ . Our task is to compute  $I$ . From Eq. 18, we have

$$I \propto \frac{\Gamma(y_0)e^{U(y_0)} - \Gamma(L)e^{U(L)}}{\int_{y_0}^L dy e^{U/K_B T}}, \quad (20)$$

where  $L$  is the system size and  $y_0$  is a short distance cutoff. At low temperature, to form a VAV with large separation, there is a large energy barrier to overcome. Thus to leading order in  $1/L$ , we expect  $\Gamma(L \rightarrow \infty) = 0$ . So we have

$$I \propto \frac{1}{\int_{y_0}^L dy e^{U/K_B T}}. \quad (21)$$

Because there are three phases in this system, there are three effective potentials and resulting resistances to consider.

### A. Linearly Confined Phase

For the weakest fluctuations (lowest temperatures), we may ignore any screening effects of the vortices on their mutual interactions. As discussed above, this leads to a phase in which a VAV pair is effectively connected by a string of overturned phase, generating an

interaction for highly separated VAV pair that grows linearly with separation. An effective potential that describes this situation in the presence of a current  $j$  is

$$\begin{aligned} U &= \varepsilon_0 \ln(r/a) + \varepsilon_1 r/a - \gamma jr \\ &= \varepsilon_0 \ln(r/a) - \Delta r, \end{aligned} \quad (22)$$

where  $\Delta = \gamma j - \varepsilon_1/a$ ,  $\varepsilon_1$  is the string free energy per unit length, and  $j$  is the current. The  $\gamma jr$  term is introduced to account for the force on a vortex due to the current. Because of this, there is a critical current  $j_c = \frac{\varepsilon_1}{a\gamma}$ . There are two cases to consider:

(i)  $j > j_c$ ,  $\Delta > 0$ . In this situation there is a critical VAV separation  $r_c = \varepsilon_0 a/\Delta$ , for which the potential  $U(r)$  increases with increasing  $r$  for  $r < r_c$ , and decreases with increasing  $r$  for  $r > r_c$ . VAV pairs with separation shorter than  $r_c$  tend to shrink, while VAV pairs with separation larger than  $r_c$  tend to increase the separation, eventually becoming free vortices. For system size  $L \gg r_c$ , a saddle point approximation leads to

$$\begin{aligned} I &\sim e^{-U(r_c)/k_B T} \\ &\sim \Delta^{\varepsilon_0/k_B T}. \end{aligned} \quad (23)$$

From Ohm's law, the interlayer voltage generated then takes the form

$$V = \rho j \sim j(j - j_c)^{\varepsilon_0/2k_B T}. \quad (24)$$

(ii)  $j < j_c$ ,  $\Delta < 0$ . In this regime, the potential  $U(r)$  increases monotonically to infinity. Thus for infinite system, the VAV pairs have to overcome an infinite high barrier to become free vortices. We expect no free vortices for an infinite system. In finite size systems, we expect corrections to this, which may be estimated as follows.

$$\begin{aligned} I &\sim \frac{1}{\frac{k_B T}{-\Delta} \left(\frac{r}{a}\right)^{\varepsilon_0/k_B T} e^{-r\Delta/k_B T} \Big|_{x_0}^L + \int_{x_0}^L e^{-r\Delta/k_B T} \left(\frac{r}{a}\right)^{(\varepsilon_0/k_B T - 1)} dr} \\ &\sim \frac{1}{\frac{k_B T}{-\Delta} \left(\frac{L}{a}\right)^{\varepsilon_0/k_B T} e^{-\Delta L/k_B T}} \\ &\sim \frac{-\Delta}{k_B T} \left(\frac{a}{L}\right)^{\varepsilon_0/k_B T} e^{\Delta L/k_B T} \end{aligned} \quad (25)$$

and

$$V = j\rho \sim j \sqrt{\frac{(j_c - j)}{k_B T}} \left(\frac{a}{L}\right)^{\varepsilon_0/2k_B T} e^{-\gamma(j_c - j)L/2k_B T}. \quad (26)$$

When system size goes to infinity, the interlayer voltage disappears throughout the region  $j < j_c$ , and we have true dissipationless superconductivity. This is in contrast to single layer superconductors, which generically have a power law  $I - V$ . For current very small  $\sim 0$ , the resistivity decreases with increasing of system according to exponential law, i.e.  $\rho \sim e^{-\varepsilon_1 L/2ak_B T}$ . We will demonstrate this behavior in our simulations below.

## B. Logarithmically confined phase

In this phase, the potential for a VAV pair has the form

$$U(r) = \varepsilon_0 \ln(r/a) - \gamma jr. \quad (27)$$

There is again a critical VAV separation  $r_c = \frac{\varepsilon_0}{\gamma j}$  above which they are free. For very large system size  $L \gg r_c$ , we can apply a saddle point approximation to the integral in Eq. 21 and we find

$$V \sim \rho j \sim j^{1+\varepsilon_0/2k_B T}. \quad (28)$$

This is exactly the result of AHNS. For fixed finite system size  $L$ , we consider the situation of very small current  $j \rightarrow 0$  to obtain an Ohmic dissipation,

$$\begin{aligned} I &\sim \frac{1}{\int_{y_0}^L \left(\frac{r}{a}\right)^{\varepsilon_0/k_B T}} \\ &= (\varepsilon_0/k_B T + 1) \left(\frac{a}{L}\right)^{-(1+\varepsilon_0/k_B T)}. \end{aligned} \quad (29)$$

Thus the system size dependence of the resistivity follows a power law with system size,  $\rho \sim L^{-(1/2+\varepsilon_0/2k_B T)}$ .

## C. Free vortex phase

For the free vortex phase, in the limit of infinite system size, the density of free vortices is a constant, and we get a linear  $I - V$ ; i.e., Ohm's law. For finite system size, some bound VAV pairs with separation of order  $L$  also contribute to the voltage. Thus with increasing  $L$ , the resistivity decreases (due to the decreasing number of effectively unbound VAV pairs) and saturates to a non-zero value as  $L \rightarrow \infty$ .

## V. NUMERICAL SIMULATION

To test the results discussed above, we studied the dissipation due to vortices in Langevin dynamics simulations. The simulation models a Josephson coupled bilayer superconductor, in which we directly simulate *only the relative phase degree of freedom*. This is an important simplification because it cuts in half the computer time needed to collect data for a given set of parameters, which is often considerable. The dynamics of the angles in this system are simulated by integrating the classical equations of motion, so that our system may be understood as a variation of the resistively shunted Josephson junction model [16]. As

described below, we introduce explicit, ideal (dissipationless) leads, which are weakly coupled to each of the two edges of the system at  $x = \pm L_x/2$ . In the  $y$ -direction we adopt periodic boundary conditions. In our Langevin dynamics simulation, the equations of motion are taken to be

$$\Gamma \frac{d^2\Phi(r)}{dt^2} = \frac{\delta H_{XY}}{\delta \Phi(r)} + \zeta(r) - \eta \frac{d\Phi(r)}{dt}. \quad (30)$$

Here  $\Phi(r)$  include the phase difference for the two layers and the two leads. Following Ref. 16, we apply a “busbar geometry” in which there is a *single* phase variable in each of the leads. This eliminates the possibility of vortices in the leads themselves, and allows us to focus on dissipation due only to the system. In practice, this might be accomplished by using superconducting films for the leads that are much thicker than those of the system, so that they will have a much higher superfluid stiffness [17] than inside the system itself. An important aspect of the simulation is that the coupling between the system and the leads must be *weak* to avoid disturbing the behavior of vortices that approach the edge. For the results reported here, we took  $K_L = K_R = 0.05$  (see below) whereas the coupling within the system was taken as  $K = 1$ , setting our unit of energy. The effective moment of inertial for the spins were also taken to be 1. The viscosity  $\eta$  was taken to be 0.143 in our simulation.  $\zeta(r)$  is a random torque satisfying  $\langle \zeta(r, t)\zeta(r', t') \rangle = 2\eta T \delta_{r,r'} \delta(t - t')$  with  $T$  being the temperature of the system (chosen to be 1.2 for the results discussed below.) For a system of size  $N_x, N_y$ , our Hamiltonian  $H_{XY}$  takes the form

$$\begin{aligned} H_{XY} = & -K \sum_{\langle r,r' \rangle} \cos[\Phi(r) - \Phi(r')] - h \sum_r \cos[\Phi(\mathbf{r})] \\ & -K_L \sum_{j=1}^{N_y} \cos(\Phi_L - \Phi(a\hat{x} + aj\hat{y})) - K_R \sum_{j=1}^{N_y} \cos(\Phi_R - \Phi(N_x a\hat{x} + aj\hat{y})) \end{aligned} \quad (31)$$

with  $K = 1$ . A typical run consists of  $3.9 \times 10^8$  time steps. Each time step is 0.08 (in the unit of  $\sqrt{\Gamma/K}$ ). We also eliminate the initial  $1.5 \times 10^7$  steps in these runs for equilibration. We repeated runs for each set of parameters with several different seeds, allowing us to estimate the statistical error.

In principle, we can find the resistances and I-V curves by injecting counterflow current, which in this model would act as a constant force on the lead phase variables  $\Phi_L$  and  $\Phi_R$ . The induced interlayer voltage is then just given by the Josephson relation,  $V_{L,R} \propto d\Phi_{L,R}/dt$ . However, for low currents such simulations become very challenging because there are long time scales involved. To simplify our calculation, instead of calculating the  $I - V$  curves directly, we calculate the resistance for small current ( $j \rightarrow 0$ ) via the Einstein relation. The response of a lead variable  $\Phi_{L,R}$  to a DC driving force (current) is proportional to its diffusion constant, which can be calculated by the correlation function

$$D = \lim_{T \rightarrow \infty} \frac{1}{T} \langle (\Phi'(t+T) - \Phi'(t))^2 \rangle_t, \quad (32)$$

where, for example,  $\Phi' = \Phi_L - \Phi_0$ , and  $\Phi_0$  is a spin angle at some point deep inside the system. Here we choose it to be the middle point of the sample.  $\langle \dots \rangle_t$  refers to an

average over different starting times, which is essentially an average over initial conditions. Because in our model current acts as a driving force and voltage is an average velocity of the lead phases in response, the diffusion constant for the lead variables are proportional to the *resistance* of the system.

Our simulation results are summarized in Fig. 2. We show the system size ( $N_y$ ) dependence of the diffusion constant (i.e. resistance) for  $h=0.0286, 0.143, 1.43$ . Our system size is  $N_x = 29$  (fixed) and  $N_y=40,50,60,75,85$ . It is clear that there are three different behaviors. The curve with solid dots is for  $h = 0.0287$ , which shows a straight line with slope very close to -1. Here the dashed line is a reference line with slope exactly -1. The resistance  $R \sim N_y^{-1}$  comes purely from the geometry of the sample and implies a constant *resistivity* (i.e.,  $R = \rho N_x/N_y$ ). Thus this result is consistent with the system being in the free vortex phase. The curve with solid squares for  $h = 0.143$  is a straight line with slope  $> 1$  on the log-log plot of Fig. 2, indicating that the system size dependence of the resistivity has a power law behavior. This is consistent with our expectations for the logarithmically confined vortex phase. Finally, the curve with solid triangle for  $h = 1.43$  shows a marked downward curvature on the log-log plot. In the insert, this curve is shown in a log-linear plot, demonstrating a nice exponential law for the system size dependence. This is consistent with our expectations for the linearly confined phase. Thus our numerical results show that for a fixed temperature  $T > T_{KT}$ , with increasing  $h$  (interlayer tunneling), the resistance has three different possible qualitative behaviors.

## VI. CONCLUSION

By a combination of analytical analysis and numerical simulation, we have shown that a bilayer thin film superconductor supports three vortex phases for the antisymmetric combination of the layer phase variables: a free vortex phase, a logarithmically confined phase, and a linearly confined phase. We argued from a Fokker-Planck analysis that the corresponding interlayer  $I - V$  curves should show measurably different behaviors: metallic conductivity for the unbound phase, a power law  $I - V$  in the logarithmically bound phase, and true dissipationless superconductivity (for an infinite system) in the linearly confined phase. We demonstrated that this behavior is consistent with what is found in numerical simulations.

**Acknowledgments** The authors would like to acknowledge discussions with Steve Girvin in the early stages of this work. This research was supported by NSF Grant Nos. DMR-

- [1] L. P. Kadanoff, *Statistical Physics: Dynamics, Statics, and Renormalization* (World Scientific, Singapore, 2000).
- [2] N. D. Mermin and H. Wagner, Phys. Rev. Lett. 17, 1133 (1966). P. C. Hohenberg, Phys. Rev. 158, 383 (1967).
- [3] J. M. Kosterlitz, D. Thouless, J. Phys. C 6, 1181 (1973); J. M. Kosterlitz, J. Phys. C 7, 1046 (1974).
- [4] H. A. Fertig, Phys. Rev. Lett. 89, 035703 (2002).
- [5] H. A. Fertig and Kingshuk Majumdar, Ann. Phys. 305, 190 (2003).
- [6] H. A. Fertig and Joseph P. Straley, Phys. Rev. B. **66**, 201402(R) (2002).
- [7] B. I. Halperin and David Nelson, J. Low Temp. Phys. 36, 599 (1979).
- [8] R. A. Ferrell and R. E. Prange, Phys. Rev. Lett. 10, 479 (1963).
- [9] W.E. Lawrence and S. Doniach, in *Proceedings of the Twelfth International Conference on Low Temperature Physics*, (Academic Press of Japan, Kyoto, 1971).
- [10] N. Parga and J. E. Van Himbergen, Solid State Commun. 35, 607 (1980); N. Parga and J. E. Van Himbergen, Ann. Phys. (N. Y.) 134, 286 (1981).
- [11] J. V. José, L. P. Kadanoff, S. Kirkpatrick, and D. R. Nelson, Phys. Rev. B **16**, 1217 (1977).
- [12] J. Villain, J. Phys. **36**, 581 (1975).
- [13] J. Cardy, *Scaling and Renormalization in Statistical Physics*, (Cambridge, New York, 2000).
- [14] S. M. Girvin and A. H. MacDonald, *Multicomponent Quantum Hall Systems: The Sum of Their Parts and More*, in Perspectives in Quantum Hall Effects, edited by S. Das Sarma and A. Pinczuk, (Wiley, New York, 1997).
- [15] V. Ambegaokar, B. I. Halperin, D. R. Nelson, and E. D. Siggia, Phys. Rev. B 21, 1806 (1980).
- [16] M. V. Simkin and J. M. Kosterlitz, Phys. Rev. B 55, 11646 (1997).
- [17] S.M. Girvin, private communication.

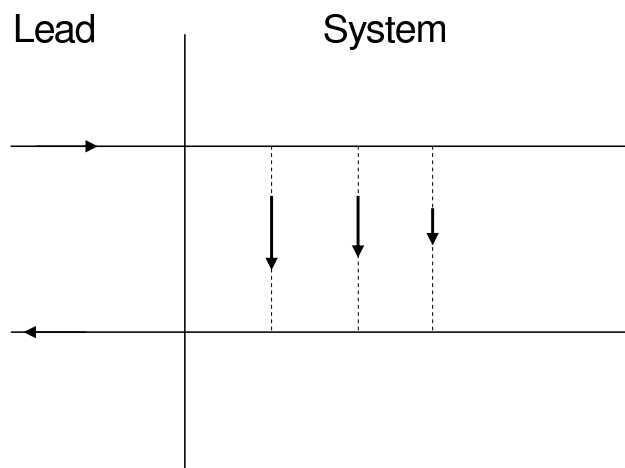


FIG. 1: Bilayer system with current being injected and removed from the two layers at the same edge by an ideal lead.



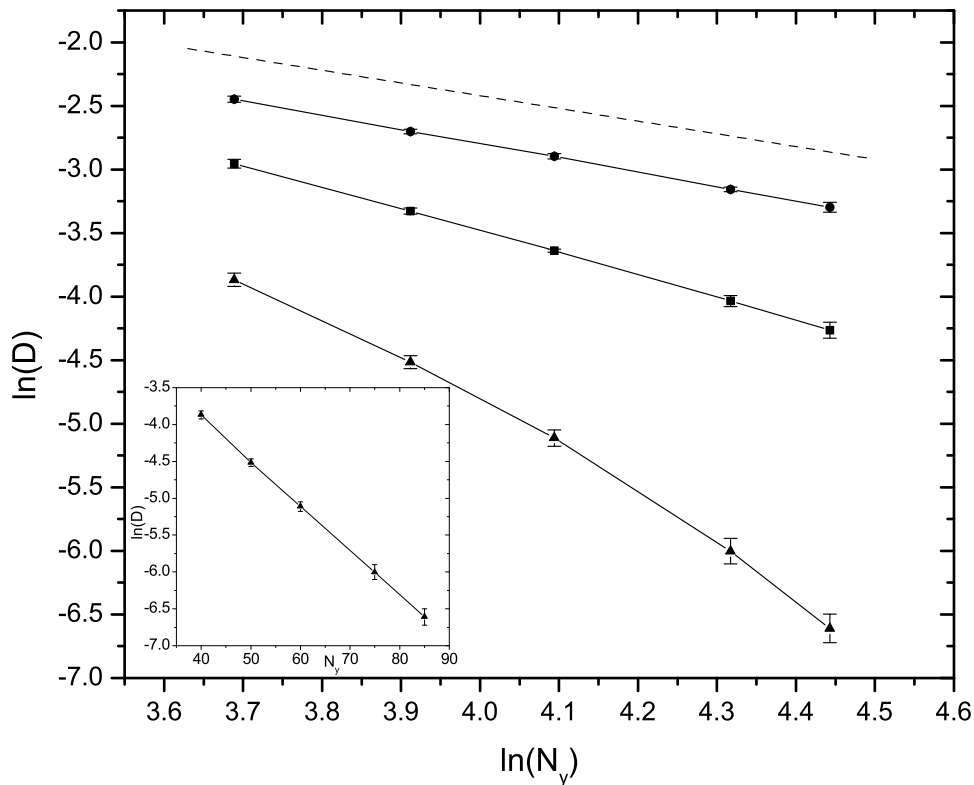


FIG. 2: The diffusion constant vs. system size  $N_y$  in a log-log plot with error bars.  $N_x = 29$  is fixed. The curve with solid dots is for  $h = 0.0286$ , corresponding to the free vortex phase, showing  $D(\sim R) \sim N_y^{-1}$ . The dashed line is the reference line with slope -1. The curve with solid squares is for  $h = 0.143$ , corresponding to logarithmically confined phase, showing  $D(\sim R) \sim N_y^{-a}$ ,  $a = 1.74 > 1$ , a power law  $N_y$  dependence. The curve with solid triangles is for  $h = 1.43$ , corresponding to linear confined phase. The insert shows the data for  $h = 1.43$  in a log-linear plot, clearly demonstrating the exponential system size dependence.